Thermochimica Acta, 171 (1990) 229–238
Elsevier Science Publishers B.V., Amsterdam

CRYSTALLINE STRUCTURE AND THERMAL STABILITY OF DOUBLE STRONTIUM AND BARIUM CARBONATES

J.M. CRIADO, M.J. DIANEZ and M. MACIAS

Instituto de Ciencia de Materiales, Centro Mixto Universidad de Sevilla C.S.I.C., Apdo. 1115, 41071 Sevilla (Spain)

M.C. PARADAS

Dpto. Quimica Inorgánica, Facultad de Quimica de la Universidad Complutense, Ciudad Universitaria, 28040 Madrid (Spain)

(Received 28 March 1990)

ABSTRACT

The crystalline structures of double salts of composition $Sr_xBa_{1-x}CO_3$ have been analysed. It has been shown that this series of compounds crystallizes in the orthorhombic system over the entire composition range. Moreover, they conform to Veghard's law.

The thermal decomposition of a series of samples of composition $Sr_xBa_{1-x}CO_3$ ($x = 0.2$, 0.4, 0.5, 0.6 and 0.8) has been studied by means of the constant rate thermal analysis (CRTA) technique. This method permits monitoring of the vacuum and the sample temperature in such a way that both the pressure in the close vicinity of the sample and the total decomposition rate remain constant over the whole reaction range. The results obtained at a CO_2 residual pressure of 4×10^{-5} Torr show that the thermal decomposition of BaSr double salts takes place in a single step, instead of the two step process previously claimed in the literature. The comparative kinetic analysis of both CRTA and TG curves at high vacuum has allowed the reaction mechanism and the activation energy for the process to be established.

INTRODUCTION

Mixed carbonates of calcite–aragonite structure have been widely employed for the synthesis of mixed oxides used as catalysts [1,2] or in the manufacture of cathode coatings [3,4]. Fubini and Stone [5] have recently shown that $MnCO_3$–$CaCO_3$ forms solid solutions over the full composition range. Ostapchenko [4] reported that $CaCO_3$–$SrCO_3$ forms solid solutions over the 0–100% range. However, Stone [1] has concluded in a recent paper from crystallographic studies that the single phase $Sr_xCa_{1-x}CO_3$ does not precipitate at $0.2 < x < 0.5$. Several authors [3,6,7] have observed that the DTA diagrams for coprecipitated Sr–Ba carbonates show a reversible peak that moves, as a function of the composition range, from 900 °C in pure $BaCO_3$ to 800 °C in pure $SrCO_3$, reaching a minimum at the composition $0.4BaCO_3 \cdot 0.6SrCO_3$. Moreover, Judd and Pope [3] observed that the tem-

0040-6031/90/$03.50

peratures of the DTA peaks of $SrCO_3$ and $BaCO_3$ roughly correspond with the temperature of the orthorhombic–hexagonal transformation of these carbonates. Therefore they concluded that the mixed Sr–Ba carbonates form solid solutions over the full compositional range, and they assign the DTA peak to an orthorhombic–hexagonal polymorphic transformation of the double salts. However, it is noteworthy that crystallographic data for these materials have not yet been reported.

The mechanism of the thermal decomposition of mixed carbonates of calcite–aragonite structure has merited the attention of a number of authors [8,9]. They have concluded that even under vacuum [9] the reaction takes place in two stages; the first one gives oxide and the most basic carbonate, and the second corresponds to the thermal decomposition of this carbonate. However, it is necessary to take into account that it has not been checked in previous papers whether the experimental conditions used allow proper removal of the CO_2 generated in the reaction. Therefore, the carbonate obtained in the first stage of the thermal decomposition of the mixed carbonates could be formed from a secondary reaction between CO_2 and the most basic oxide. The thermal decomposition of Sr–Ba double carbonates has been studied in the present paper by means of the recently developed constant rate thermal analysis (CRTA) technique [10] in order to avoid mass transfer phenomena. This permits, in principle, monitoring at the desired value of both the CO_2 pressure in the close vicinity of the sample and the total decomposition rate over the whole reaction range.

EXPERIMENTAL

Materials

Analytical reagent grade $Sr(NO_3)_2$, $Ba(NO_3)_2$ and $(NH_4)_2CO_3$ (Riedel) were used.

A series of samples of composition $Sr_xBa_{1-x}CO_3$ ($x = 0.2$, 0.4, 0.5, 0.6 and 0.8) was prepared. Appropriate quantities of $Sr(NO_3)_2$ and $Ba(NO_3)_2$, in the required Sr : Ba ratio, were dissolved in distilled water. A large excess of a 1 M solution of $(NH_4)_2CO_3$ was then added rapidly into the nitrate solution at 90 °C, with rapid stirring. The precipitate was filtered off, washed with cold distilled water and dried in air at 110 °C for 48 h and at 400 °C for 4 h.

Methods

The X-ray diffraction diagrams of the samples were recorded with a Siemens diffractometer using Cu $K\alpha$ radiation and a graphite monochroma-

tor. Pure silicon was used as internal standard for a precise determination of 2θ diffraction angles. The values of a, b and c for the orthorhombic cell, determined from Veghard's law, were used as starting parameters in the Lsucre method for refining the lattice parameters.

A Mettler Thermoanalyzer with a platinum crucible 16 mm in diameter was employed. The apparatus has been modified in order to monitor the furnace temperature in such a way that the total decomposition rate remains constant over the whole decomposition range. This has been attained by both controlling the residual pressure in the close vicinity of the sample and maintaining a constant value of the pumping rate, which can be selected by means of a butterfly valve. The Thermoanalyzer has been modified without impairing its original performance; therefore it is also possible to record TG diagrams.

RESULTS AND DISCUSSION

Determination of the lattice parameters

The X-ray diffraction diagrams of the Sr–Ba carbonates show that these compounds are made up of well crystallized single phases of orthorhombic structure; i.e. aragonite structure. The d-spacing and the relative intensities of the maximum diffraction lines are included in Tables 1 to 5 with their corresponding (hkl) indices. The lattice parameters and the volumes of the unit cells, V_0, are collected in Table 6. The plot of V_0 versus the barium percentage of the mixed carbonate, included in Fig. 1, shows that Veghard's law is obeyed.

TABLE 1

X-ray powder diffraction pattern of $Sr_{0.2}Ba_{0.8}CO_3$

$h\,k\,l$	d	I/I_0	$h\,k\,l$	d	I/I_0
1 1 0	4.528	46	2 0 2	2.029	9
0 2 0	4.412	18	1 3 2	1.996	18
1 1 1	3.691	94	2 3 1	1.873	2
0 2 1	3.632	52	2 2 2	1.843	3
2 0 0	3.624	53	3 1 0	1.723	6
1 3 0	2.566	100	2 4 0	1.690	7
2 2 0	2.259	36	3 1 1	1.661	15
0 4 0	2.200	12	1 5 1	1.616	13
2 2 1	2.130	60	3 3 0	1.510	13
0 4 1	2.082	26			

TABLE 2

X-ray powder diffraction pattern of $Sr_{0.4}Ba_{0.6}CO_3$

h k l	*d*	I/I_0	*h k l*	*d*	I/I_0
1 1 0	4.478	33	2 2 1	2.107	55
0 2 0	4.354	12	0 4 1	2.055	33
1 1 1	3.648	100	2 0 2	2.099	10
0 2 1	3.586	48	1 3 2	1.975	17
2 0 0	2.609	35	1 1 3	1.898	8
1 3 0	2.535	72	2 2 2	1.823	4
1 3 1	2.344	5	3 1 0	1.706	5
2 2 0	2.239	25	2 4 0	1.669	6
0 4 0	2.179	9	3 1 1	1.648	14

TABLE 3

X-ray powder diffraction pattern of $Sr_{0.5}Ba_{0.5}CO_3$

h k l	*d*	I/I_0	*h k l*	*d*	I/I_0
1 1 0	4.447	15	2 2 1	2.097	32
0 2 0	4.325	6	0 4 1	2.047	27
1 1 1	3.629	100	2 0 2	1.999	22
1 2 1	2.936	50	1 3 2	1.966	9
2 0 0	2.596	40	3 3 0	1.486	6
1 3 0	2.525	36	3 3 2	1.341	6
2 2 0	2.230				

TABLE 4

X-ray powder diffraction pattern of $Sr_{0.6}Ba_{0.4}CO_3$

h k l	*d*	I/I_0	*h k l*	*d*	I/I_0
1 1 0	4.441	18	0 4 0	2.159	7
0 2 0	4.328	8	2 2 1	2.092	52
1 1 1	3.620	100	0 4 1	2.030	20
0 2 1	3.567	55	1 3 2	1.954	18
1 2 1	2.931	4	2 2 2	1.875	9
2 0 0	2.592	28		1.809	4
1 3 0	2.519	62	3 1 1	1.626	12
2 2 0	2.225	21	2 4 1	1.584	11

TABLE 5

X-ray powder diffraction pattern of $Sr_{0.8}Ba_{0.2}CO_3$

h k l	*d*	I/I_0	*h k l*	*d*	I/I_0
1 1 0	4.397	14	2 2 1	2.071	60
1 1 1	3.566	100	0 4 1	2.014	22
0 0 2	3.053	45	1 1 3	1.851	8
1 2 1	2.886	4	2 2 2	1.788	4
2 0 0	2.564	30	0 5 0	1.702	12
0 2 2	2.485	70	2 4 1	1.585	10
2 2 0	2.200	30	1 5 1	1.564	11
0 4 0	2.130	8	1 0 4	1.466	11

TABLE 6

Lattice parameters (Å) and volumes (Å^3) of the unit cells

Sample	*a*	*b*	*c*	*V*
$Sr_{0.2}Ba_{0.8}CO_3$	5.248(2)	8.841(3)	6.357(3)	296.9(1)
$Sr_{0.4}Ba_{0.6}CO_3$	5.220(3)	8.707(4)	6.287(4)	285.8(1)
$Sr_{0.5}Ba_{0.5}CO_3$	5.195(2)	8.665(5)	6.258(8)	281.7(3)
$Sr_{0.6}Ba_{0.4}CO_3$	5.164(2)	8.604(4)	6.187(3)	279.9(3)
$Sr_{0.8}Ba_{0.2}CO_3$	5.137(3)	8.118(3)	6.118(3)	267.8(2)

Thermal decomposition of Sr–Ba carbonates

Figure 2 shows, by way of example, a series of TG curves of $Sr_{0.6}Ba_{0.4}CO_3$ obtained using different sample sizes and heating rates. It can be observed that the decomposition reaction takes place in a single stage if both sample size and heating rate are sufficiently low. Otherwise, the reaction occurs in two stages, as shown in Fig. 2. X-ray diffraction analysis of the partially decomposed $Sr_{0.6}Ba_{0.4}CO_3$ shows that a single phase of orthorhombic carbonate is obtained if the thermal decomposition is carried out as described for Fig. 2a, while $Sr_{0.6}Ba_{0.4}CO_3$ and $BaCO_3$ result if the thermal decomposition of the double carbonate occurs as shown in Fig. 2b. Therefore, it can be concluded that the thermal decomposition of Sr–Ba carbonates takes place in a single stage yielding the corresponding oxides and CO_2. However, if the CO_2 is not efficiently removed from the close vicinity of the sample, a secondary reaction with BaO would yield $BaCO_3$, which would then decompose in a second stage according to Fig. 2b.

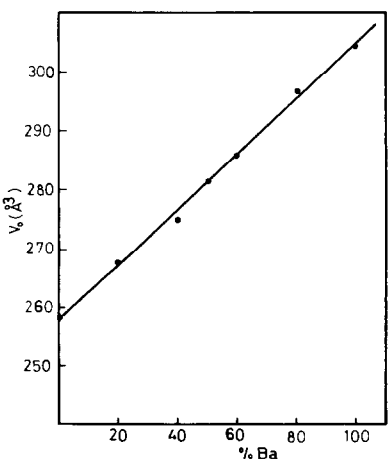

Fig. 1. Plot of the unit cell volume as a function of the composition of the sample $Sr_xBa_{1-x}CO_3$.

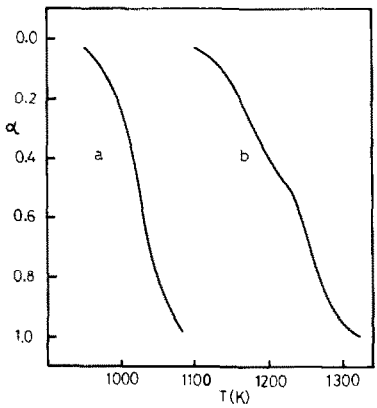

Fig. 2. Influence of sample weight and heating rate on the shape of the TG curve of $Sr_{0.6}Ba_{0.4}CO_3$. a, $w = 3.55$ mg, $\beta = 0.5\,^{\circ}C\ min^{-1}$; b, $w = 50$ mg; $\beta = 4\,^{\circ}C\ min^{-1}$.

For obtaining the TG curves of the Sr–Ba double carbonates shown in Fig. 3, the samples were previously degassed until the best vacuum available (2×10^{-5} Torr) was reached. A heating rate of $0.5\,^{\circ}C\ min^{-1}$ and sample sizes as small as 2–3 mg were used. In this way, the pressure, continuously recorded throughout the experiment, did not exceed the initial value of 2×10^{-5} Torr. A previous paper [11] has shown that in this way mass and heat transfer effects could be overcome.

The CRTA curves of $Sr_xBa_{1-x}CO_3$ included in Fig. 4 were recorded using a constant CO_2 residual pressure of 4×10^{-5} Torr, a sample size of ca. 20–30 mg and a constant decomposition rate, C, ranging from 1.2×10^{-3} to 2.6×10^{-3} min^{-1}. These experimental conditions allow heat and mass transfer phenomena to be avoided, as shown elsewhere [11].

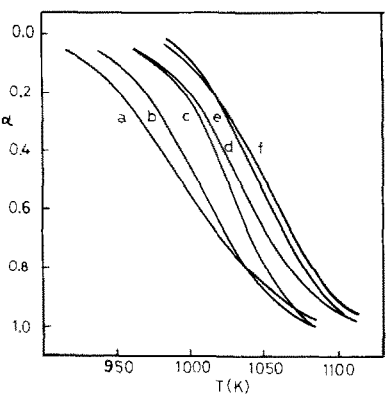

Fig. 3. TG curves for $Sr_xBa_{1-x}CO_3$ samples recorded at a heating rate $\beta = 0.5\,^{\circ}C\ min^{-1}$ and a sample weight of 3–4 mg. a, $x = 1.0$; b, $x = 0.8$; c, $x = 0.6$; d, $x = 0.4$; e, $x = 0.2$; f, $x = 0$.

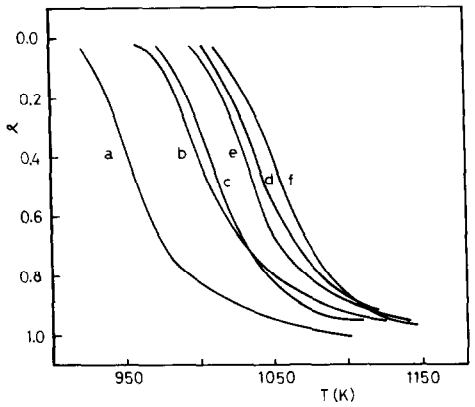

Fig. 4. CRTA curves for $Sr_xBa_{1-x}CO_3$ samples: a, $x = 1.0$, $C = 1.2 \times 10^{-3}$ min^{-1}; b, $x = 0.8$, $C = 1.4 \times 10^{-3}$ min^{-1}; c, $x = 0.6$, $C = 1.2 \times 10^{-3}$ min^{-1}; d, $x = 0.4$, $C = 2.6 \times 10^{-3}$ min^{-1}; e, $x = 0.2$, $C = 1.2 \times 10^{-3}$ min^{-1}; f, $x = 0$, $C = 1.2 \times 10^{-3}$ min^{-1}.

The procedure for performing the kinetic analysis of CRTA curves has been developed elsewhere. As is well known, the general expression for the rate of thermal decomposition reaction of a solid is

$$d\alpha/dt = A \exp(-E/RT) f(\alpha) \tag{1}$$

where α is the degree of completeness of the reaction, $f(\alpha)$ is a function depending on the reaction mechanism and the other parameters have their usual meaning. The symbols given by Sharp and Wentworth [12] will be used for naming the $f(\alpha)$ function corresponding to the different kinetic models proposed in the literature for describing solid state reactions.

Bearing in mind that CRTA diagrams are obtained at a constant decomposition rate, $C = d\alpha/dt$, eqn. (1) becomes:

$$\ln 1/f(\alpha) = \ln(A/C) - (E/RT) \tag{2}$$

Therefore, the kinetic parameters of the reaction can be obtained from the plot of the left-hand-side of eqn. (2) vs. the reciprocal of the temperature.

The analysis of the TG diagrams of Fig. 2 has been carried out by the Coats and Redfern method [13]

$$\ln g(\alpha) - 2 \ln T = \ln(AR/E_\beta) - (E/RT) \tag{3}$$

where β is the heating rate and $g(\alpha)$ is a function depending on the reaction mechanism and connected with the function $f(\alpha)$ through the expression

$$g(\alpha) = \int_0^\alpha d\alpha/f(\alpha) \tag{4}$$

The plot of the left hand side of eqn. (3) versus the reciprocal of the temperature should be a straight line from whose slope and intercept the kinetic parameters could be obtained.

TABLE 7

Kinetic parameters of the thermal decomposition of $Sr_{0.8}Ba_{0.2}CO_3$ calculated from TG and CRTA curves by assuming different kinetic laws

Mechanism	TG ($\beta = 0.5\,^{\circ}C\ min^{-1}$)			CRTA ($C = 1.4\times10^{-3}\ min^{-1}$)		
	E (kJ mol^{-1})	A (min^{-1})	Regression coefficient	E (kJ mol^{-1})	A (min^{-1})	Regression coefficient
R_2	167	2.4×10^{6}	−0.9910	92	1.1×10^{2}	−0.9999
R_3	180	1.5×10^{7}	−0.9940	121	6.4×10^{3}	−0.9999
F_1	209	8.7×10^{8}	−0.9978	192	5.0×10^{7}	−0.9999
A_2	196	3.1×10^{5}	−0.9974	84	2.5×10^{2}	−0.9364
A_3	180	5.4×10^{1}	−0.9968	50	2.6×10^{-3}	−0.7577
D_1	276	8.1×10^{11}	−0.9800	255	4.2×10^{9}	−0.9031
D_2	318	1.1×10^{14}	−0.9878	201	2.6×10^{7}	−0.9526
D_3	376	3.8×10^{16}	−0.9946	297	5.8×10^{11}	−0.9765
D_4	339	2.8×10^{14}	−0.9905	234	3.1×10^{8}	−0.9642

In a previous paper [14] it was proved theoretically that the kinetic analysis of two thermoanalytical curves obtained with a linear heating programme and the CRTA technique, respectively, would provide an excellent procedure for establishing the correct mechanism of solid state reactions. This is because a good agreement between the kinetic parameters determined from both techniques is obtained only when the kinetic equations of the actual reaction mechanism are used for performing the calculations. Accordingly, the kinetic analysis of the CRTA and the TG curve for the sample $Sr_{0.2}Ba_{0.8}CO_3$, included in Figs. 3 and 4 has been carried out by means of eqns. (1) and (3), respectively, after substituting the $f(\alpha)$ and $g(\alpha)$ functions of the mechanism of solid state reactions more usually employed in the literature.

The results obtained are included in Table 7. We can see that both a reasonable good agreement between the kinetic parameters calculated from TG and CRTA diagrams and satisfactory regression coefficients are obtained only if it is assumed that the reaction follows first order kinetics (F_1 mechanism).

Similar results have been obtained by analysing CRTA and TG curves of all the other Sr–Ba double carbonate samples studied in the present paper. The activation energies and the Arrhenius pre-exponential factors calculated from the CRTA curves in Fig. 4, assuming an F_1 kinetic model, are included in Table 8. This table also includes, for comparison, the kinetic parameters determined by Criado et al. [15] for the thermal decomposition of $SrCO_3$ and $BaCO_3$ following the method described here.

The results reported seem to show rather clearly that the thermal decomposition of Sr–Ba double carbonates takes place through a single step, contrary to previous statements in the literature [8,9]. In fact, a single step is

TABLE 8

Kinetic analysis of CRTA curves of Sr–Ba double carbonates assuming a first order law

Sample	E (kJ mol^{-1})	A (min^{-1})
$SrCO_3$	188	4.8×10^{7}
$Sr_{0.8}Ba_{0.2}CO_3$	192	5.0×10^{7}
$Sr_{0.6}Ba_{0.4}CO_3$	247	3.3×10^{10}
$Sr_{0.4}Ba_{0.6}CO_3$	213	3.6×10^{8}
$Sr_{0.2}Ba_{0.8}CO_3$	222	3.0×10^{8}
$BaCO_3$	276	1.0×10^{11}

observed in both CRTA and TG diagrams shown in Figs. 3 and 4, and a very good fit of the experimental data to the kinetic equation of a single reaction mechanism has been obtained.

Data in Table 8 seem to indicate that the activation energies for the thermal decomposition of the series of samples $Sr_xBa_{1-x}CO_3$ increase on increasing the amount of Ba^{2+} in the double salt with the exception of only the sample $Sr_{0.6}Ba_{0.4}CO_3$, which gives a value somewhat higher than would be expected. In order to explain the anomalous behaviour of this sample it is necessary to consider that Sr–Ba double carbonates undergo an orthorhombic–hexagonal phase change ($\alpha \rightleftharpoons \beta$) at a temperature depending on the Sr : Ba ratio in the sample [3,7]. A plot of the temperature of the phase change against the percentage of Ba^{2+} follows a curve which passes through a minimum (700–750 °C) at a composition close to 40 mol% of barium carbonate. The phase change temperature of this last sample is below the temperature range at which its thermal decomposition is recorded in the current paper. In other words, it may be possible that the sample with a Sr : Ba ratio of 0.6 : 0.4 has an hexagonal structure when it undergoes thermal decomposition while the others have an orthorhombic structure. The anomalous behaviour of $Sr_{0.6}Ba_{0.4}CO_3$ could perhaps then be interpreted by considering that the activation energy for the thermal decomposition of the hexagonal structure of Sr–Ba double carbonates might be somewhat higher than the corresponding energy for the orthorhombic phase.

REFERENCES

1 F.S. Stone and M.M. Ramirez de Agudelo, Proc. 9th Int. Symp. on Reactivity of Solids, Elsevier Amsterdam, 1980, p. 522.
2 B. Fubini and F.S. Stone, J. Chem. Soc., Faraday Trans. 1, 79 (1983) 1215.
3 M.D. Judd and M.I. Pope, J. Appl. Chem. Biotechnol., 21 (1971) 285.
4 E.P. Ostapchenko, Izv. Akad. Nauk SSSR, Ser. Fiz., 20 (1956) 1105.
5 B. Fubini and F.S. Stone, in P. Barrett and L.C. Dufour (Eds.), Proc. 10th Int. Symp. on Reactivity of Solids, Elsevier Amsterdam, 1985, p. 85.

6 M.D. Judd and M.I. Pope, J. Appl. Chem. Biotechnol., 21 (1971) 149.
7 J.M. Criado, C. Barriga and J. Morales, Bol. Soc. Esp. Ceram. Vidrio, 22 (2) (1983) 77.
8 M.E. Garcia-Clavel, F. Buriel-Marti and M. Rodriguez de la Peña; Inf. Quim. Anal. Pura Apl. Ind., (1970) 31.
9 M.D. Judd and M.I. Pope, in R.F. Schucanker and P.D. Carn (Eds.), Proc. 2nd Int. Conf. on Thermal Analysis, Academic Press, New York, 1969, p. 1423.
10 J. Rouquerol, J. Therm. Anal., 5 (1973) 203.
11 J.M. Criado, F. Rouquerol and J. Rouquerol, Thermochim. Acta, 38 (1980) 109.
12 J.M. Sharp and S.A. Wentworth, Anal. Chem., 41 (1969) 2050.
13 A.W. Coats and J.P. Redfern, Nature, 201 (1964) 68.
14 J.M. Criado, A. Ortega and F.J. Gotor, Thermochim. Acta, 38 (1980) 171.
15 J.M. Criado, F. Rouquerol and J. Rouquerol, Thermochim. Acta, 38 (1980) 117.